Eur. Phys. J. D **2**, 245–252 (1998)

THE EUROPEAN PHYSICAL JOURNAL D

Memory effects in speed-changing collisions and their consequences for spectral lineshape: I. Collision regime

D. Robert[a] and L. Bonamy

Laboratoire de Physique Moléculaire[b], Faculté des Sciences, La Bouloie, Université de Franche-Comté, 25030 Besancon Cedex, France

Received: 9 February 1998 / Accepted: 30 March 1998

Abstract. A consistent approach to the lineshape in the binary collision regime accounting for speed-changing collisions based on a convenient memory function is proposed. The consequences of memory effects on the spectral lineshape, through speed-dependent line broadening and line shifting mechanisms, are studied in detail for the prototype H_2-Ar system. The connection between the present memory approach and the analytical model SC + D ("speed changing" and "dephasing" collisions) based on the hard collision approximation is displayed.

PACS. 34.10.+x General theories and models of atomic and molecular collisions and interactions (including statistical theories, transition state, stochastic and trajectory models, etc.) – 33.70.Jg Line and band widths, shapes, and shifts

1 Introduction

In the impact regime, for densities significantly larger than those relevant to the Doppler regime, experimental proof was given [1] for an inhomogeneous broadening of the H_2 vibrational Q-lines in a heavy perturber gas. A simple hard collision model accounting for uncorrelated speed-changing collisions (SC) and dephasing (D) ones was proposed by Farrow *et al.* [1]. It permits a consistent description of the observed asymmetric features and of important deviations *versus* concentration from the usual linear mixing rule for the broadening coefficient in gas mixtures. This model includes the collisionally induced interferences between the various speed classes, leading in this case to a narrowing of the line with respect to a Boltzmann weighted sum of Lorentzian profiles corresponding to each class. A generalization [2] of this model accounting for partial correlations between speed-changing and dephasing mechanisms was successfully applied to an exhaustive analysis of Raman Q-lines of H_2 perturbed by various rare gases [3,4] and nitrogen [5].

These models [1,2] are based on the hard collision (HC) approximation [6,7] assuming that each collision thermalizes the radiator speed (*i.e.* the velocity modulus). In other words, no memory of this speed is preserved after each collision. The HC approximation has been extensively used [8–11] for velocity-changing (VC) collisions in order to analyze the lineshape profiles at lower densities, in the Doppler regime, by using the Rautian and Sobelman model [12]. Notice that, in the following, the Doppler regime must be understood as including the effect of collisions and the collision regime, as free of Doppler effect. The characteristic parameter of this model [12] is the velocity-changing rate ν^{VC} which is found [9] to be close to the dynamical friction coefficient β° calculated from the mass diffusion constant D_m, as expected. Residual discrepancies between ν^{VC} and β° are observed [8–11] (typically between a few percent and several ten percents). The origin of these discrepancies was studied by May and coworkers [13] by accounting for both collision confinement narrowing and inhomogeneous broadening, and they were attributed [13] to the width inhomogeneities due to SC collisions. Such inhomogeneities were first introduced by Berman [14] within the Voigt profile frame. This low density regime will be analyzed in paper II. In order to arrive at a clear understanding of all the mechanisms involved in the spectral lineshape in the various regimes, we will focus the present paper on the collision regime. Therefore Doppler effects will not be considered here.

In the collision regime, the speed-changing rate ν^{SC} for H_2 in heavy perturbers [1–5] has been found to be drastically lower than the velocity-changing one ν^{VC} (by about one order of magnitude). This drastic change of the characteristic rate parameter from the VC to SC collision regime suggests that it may be necessary to account for the specific speed-memory effects in the collision regime. The distinction between the orientation and the modulus (speed) of the radiator velocity in the memory process was previously considered by Nienhuis [15].

The second important feature is to point out the difference between the hard and soft collision models [12,16],

[a] e-mail: daniel.robert@univ-fcomte.fr
[b] UMR CNRS 6624

if we consider either the Doppler regime or the collision one. Nelkin and Ghatak [7] have demonstrated that these two collision models lead to close spectral distributions in the Doppler regime. This means that, in this last regime, the precise nature of the velocity memory kernel in the kinetic equation does not play a crucial role in the resulting spectral lineshape. This is no longer the case for the collision regime. Indeed, if we assume that the speed-memory is lost after each collision (*i.e.* if we take $\nu^{SC} = \nu^{VC}$), the inhomogeneities are drastically reduced, in strong disagreement with experiment. The efficiency of the interferences between the various speed classes is thus largely overestimated (*cf.* Refs. [1,3–5]). In the opposite soft collision limit [16], where a significant speed-change requires a very large number of collisions, the above mentioned interference mechanism disappears [17]. The absence of this collisionally induced speed-class exchange leads [1,3,5] to a large overestimation of both line width and asymmetry in the case of H_2 Q-lines perturbed by heavy rare gases or N_2.

The above analysis shows that the speed collision rate $\nu^{SC} \ll \nu^{VC} \approx \beta^\circ$ only accounts for the efficient collisions in the speed-exchange process. In order to obtain a unified approach for collisional, Doppler and intermediate regimes, it is necessary to introduce a memory function $f(\mathbf{v}', \mathbf{v})$ depending, not only on the outgoing velocity $\mathbf{v}$ (as in the HC assumption), but also on the incoming velocity $\mathbf{v}'$. A realistic model for such a memory function was proposed a long time ago [18] by Keilson and Storer (KS) to describe the relaxation of the translational velocity. Later, it was successfully employed in various other physical problems [19,20], in particular for the pressure-induced collapse of the rotational structure of Raman Q-lines in gases [21,22].

The main objective of this first paper is to analyze in detail the role of the translational speed-memory effect on spectral lineshapes in the collision regime, through the speed- dependence of the collisional broadening $\gamma_{coll}(v)$ and shifting $\delta_{coll}(v)$ coefficients [14]. Starting from the kinetic impact equation with the KS kernel, the expression for the lineshape is established in Section 2. Section 3 is devoted to a numerical study of the speed-memory effects on the spectral distribution with application to the prototype H_2-Ar system. A simplified memory function is proposed in Section 4 in order to obtain an analytical expression for the lineshape and to clarify the connection with the well-known hard collision limit. Concluding remarks are given in Section 5.

2 Kinetic equation and resulting lineshape

2.1 The kinetic equation with the KS speed-memory function

If we assume that the SC and D collisions are statistically independent [1,12], the kinetic impact equation for the radiating dipole characterized by speed v at time t in the collision regime is [12,2]

$$\frac{\partial}{\partial t} d(v,t) \equiv \dot{d}(v,t) = -\nu^{VC}\left[d(v,t) - \int_0^\infty f(v',v) d(v',t) dv'\right] - \left[\gamma_{coll}(v) + i\delta_{coll}(v)\right] d(v,t), \quad (1)$$

where the speed-memory function $f(v',v)$ is the average of the velocity-memory function $f(\mathbf{v}', \mathbf{v})$ over all possible orientations of $\mathbf{v}$.

Following Keilson and Storer [18], we introduce the probability per unit time that the optically active molecule, with velocity $\mathbf{v}'$, undergoes a transition to a volume $d\mathbf{v} = v^2 dv\, d\Omega$ about $\mathbf{v}$. Within the KS model, this probability is [18]

$$A(\mathbf{v}', \mathbf{v}) = \nu^{VC} f_\gamma^{KS}(\mathbf{v}', \mathbf{v}) \equiv \nu^{VC}(1-\gamma^2)^{-3/2} W_B\left(\frac{\mathbf{v} - \gamma\mathbf{v}'}{\sqrt{1-\gamma^2}}\right), \quad (2)$$

where $W_B(...)$ means the Boltzmann distribution.

After averaging over the $\mathbf{v}$-orientation, the KS speed-memory function is [22,23]

$$f_\gamma^{KS}(v',v) = \int f_\gamma^{KS}(\mathbf{v}', \mathbf{v}) d\Omega = 2\left(\frac{\tilde{\beta}}{\pi}\right)^{1/2} \frac{v}{\gamma v'} e^{-\tilde{\beta}(v^2+\gamma^2 v'^2)} \mathrm{sh}(2\tilde{\beta}\gamma v v'). \quad (3)$$

In equations (1) and (2), ν^{VC} is the velocity-changing collision frequency (assumed [12] to be $\mathbf{v}$-independent) and γ the *unique* parameter characterizing the strength of inelastic collisions in the KS model. Moreover, $(1-\gamma^2)\tilde{\beta} = m/2kT$ in equation (3), where m is the mass of the radiator and T the absolute temperature of the gas. For $\gamma = 0$, the $f_0^{KS}(v',v)$ memory function (Eq. (3)) is equal to the Boltzmann distribution $W_B(v)$. In this HC limit, the radiator speed is thermalized after each collision and its memory is completely lost. If γ is close to 1 (*i.e.* for soft collisions), the radiator speed is only slightly changed after each collision and the outgoing value v remains correlated to the incoming one v' for a time very much larger than the time between collisions. With *intermediate* values of γ, we account for physical situations where the random process is *partially correlated for the translational speed*. Our goal is to analyze the gradual transformation of an isolated absorption, emission or scattering line profile due to this partial correlation when γ_{coll} and δ_{coll} are speed-dependent.

In order to solve equation (1) with $f(v',v) = f_\gamma^{KS}(v',v)$ (*cf.* Eq. (3)), we can use the fact that the generalized Laguerre polynomials $L_n^{1/2}(mv^2/2kT) \equiv L_n^{1/2}(x)$ are eigenfunctions of the integral operator [22] in this kinetic equation

$$f_\gamma^{KS}(x',x) = \overline{W}_B(x) \sum_{n=0}^{\infty} \gamma^{2n} \overline{L}_n^{1/2}(x') \overline{L}_n^{1/2}(x), \qquad \overline{W}_B(x) = \frac{\sqrt{x} e^{-x}}{\Gamma(3/2)}, \quad (4)$$

$$\dot{a}_n(t) = -\nu^{VC}(1-\gamma^{2n})a_n(t) - \sum_{n'=0}^{\infty}\left\{\left[(1+\alpha)^{-1}\frac{T}{T_0}\right]^{r/2}[\overline{\gamma}_{coll}(T_0) - (\gamma_{coll})_0]I^{(r)}_{nn'}(\alpha) + (\gamma_{coll})_0\delta_{nn'} + i\left[(1+\alpha)^{-1}\frac{T}{T_0}\right]^{s/2}[\overline{\delta}_{coll}(T_0) - (\delta_{coll})_0]I^{(s)}_{nn'}(\alpha) + i(\delta_{coll})_0\delta_{nn'}\right\}a_{n'}(t). \quad (15)$$

where the normalized Laguerre polynomials $\overline{L}_n^{1/2}(x)$ are defined in terms of the usual ones by [23]

$$\overline{L}_n^{1/2}(x) = [n!\Gamma(3/2)/\Gamma(n+3/2)]^{1/2}L_n^{1/2}(x), \quad (5)$$

and satisfy the orthonormalization relation

$$\int_0^{\infty} dx\overline{W}_B(x)\overline{L}_n^{1/2}(x)\overline{L}_{n'}^{1/2}(x) = \delta_{nn'}. \quad (6)$$

The radiating dipole may be expanded over these (normalized) eigenfunctions

$$d(v,t) = \overline{W}_B(x)\sum_{n=0}^{\infty}a_n(t)\overline{L}_n^{1/2}(x). \quad (7)$$

Taking into account the equilibrium initial condition ($d(v,0) = W_B(v)$), we obtain from equations (1), (4) and (7) for the $\{a_n(t)\}$ coefficients

$$\dot{a}_n = -\nu^{VC}(1-\gamma^{2n})a_n(t) - \sum_{n'=0}^{\infty}a_{n'}(t)\int_0^{\infty}dx\overline{W}_B(x) \times [\gamma_{coll}(x) + i\delta_{coll}(x)]\,\overline{L}_n^{1/2}(x)\overline{L}_{n'}^{1/2}(x). \quad (8)$$

The line profile $I(\omega)$ corresponds to the equilibrium distribution in equation (7), *i.e.* to the $a_0(t)$ coefficient. Taking the Laplace transform of $d(t) = \int_0^{\infty} d(v,t)dv$,

$$d(\tilde{\omega}) = \int_0^{\infty} dt e^{i\tilde{\omega}t}d(t), \quad (9)$$

the line profile $I(\omega)$ is defined by

$$I(\omega) = \pi^{-1}\ \mathrm{Re}\{d(\tilde{\omega})\} = \pi^{-1}\ \mathrm{Re}\{a_0(\tilde{\omega})\}. \quad (10)$$

Notice that in equations (9) and (10), $\tilde{\omega}$ means the detuned frequency counted from the rovibrational frequency ω_0 of the isolated optically active molecule, $\tilde{\omega} = \omega - \omega_0$.

2.2 Line profile for speed-dependent γ_{coll} and δ_{coll}

As a first step, we will assume that the dependence of the collisional parameters γ_{coll} and δ_{coll} in equation (8) has the usual simple form $\gamma_{coll} \propto v_{rel}^r$ and $\delta_{coll} \propto v_{rel}^s$ with respect to the relative speed v_{rel} between radiator and perturber. This assumption is useful and clarifies the presentation. After a Boltzmann average over v_{rel} for a given v value, the resulting radiator speed-dependence of collisional line broadening and line shift is [24,25]

$$\gamma_{coll}(x,T) = \left[(1+\alpha)^{-1}\frac{T}{T_0}\right]^{r/2}[\overline{\gamma}_{coll}(T_0) - (\gamma_{coll})_0] \times M\left(-\frac{r}{2},\frac{3}{2};-\alpha x\right) + (\gamma_{coll})_0, \quad (11)$$

and

$$\delta_{coll}(x,T) = \left[(1+\alpha)^{-1}\frac{T}{T_0}\right]^{s/2}\left[\overline{\delta}_{coll}(T_0) - (\delta_{coll})_0\right] \times M\left(-\frac{s}{2},\frac{3}{2};-\alpha x\right) + (\delta_{coll})_0, \quad (12)$$

where $\alpha = m_p/m$ (m_p being the mass perturber), T_0 is a reference temperature, $M\,(-s/2,3/2;-\alpha x)$ is the confluent hypergeometric function [23], and the x-averaged collisional parameters $\overline{\gamma}_{coll}(T)$ and $\overline{\delta}_{coll}(T)$ are defined by

$$\begin{aligned}\overline{\gamma}_{coll}(T) &= \int_0^{\infty}dx\overline{W}_B(x)\gamma_{coll}(x,T)\\ &= \left(\frac{T}{T_0}\right)^{r/2}[\overline{\gamma}_{coll}(T_0) - (\gamma_{coll})_0] + (\gamma_{coll})_0,\\ \overline{\delta}_{coll}(T) &= \int_0^{\infty}dx\overline{W}_B(x)\delta_{coll}(x,T)\\ &= \left(\frac{T}{T_0}\right)^{s/2}\left[\overline{\delta}_{coll}(T_0) - (\delta_{coll})_0\right] + (\delta_{coll})_0, \end{aligned} \quad (13)$$

which corresponds to equations (16) and (18) of reference [3], but with an homogeneous physical redefinition of the coefficients. Introducing the following symmetric matrix elements

$$I^{(p)}_{nn'}(\alpha) = \int_0^{\infty}dx\overline{W}_B(x)M(-\frac{p}{2},\frac{3}{2};-\alpha x)\overline{L}_n^{1/2}(x)\overline{L}_{n'}^{1/2}(x), \quad p = r \text{ or } s, \quad (14)$$

equation (8) becomes

See equation (15) above

For the particular case $p = 2$, the matrix defined by equation (14) takes the exact tridiagonal form [22,23]

$$I^{(2)}_{nn'}(\alpha) = \delta_{n',n} + \frac{2}{3}\alpha\Bigg\{\left(2n+\frac{3}{2}\right)\delta_{n'n} - \sqrt{n(n+1/2)}\delta_{n',n-1} - \sqrt{(n+1)\left(n+\frac{3}{2}\right)}\delta_{n',n+1}\Bigg\}. \quad (16)$$

Of course, a more general dependence of γ_{coll} and δ_{coll} *vs.* v_{rel} (as, for instance, a linear combination [1,3] of power laws or numerical results from *ab initio* calculations) may be easily introduced. The structure of equation (15) being preserved, this equation will be rewritten in terms of a generalized $\Gamma_{nn'}$ matrix as

$$\dot{a}_n(t) = -\nu^{VC}(1-\gamma^{2n})a_n(t) - \sum_{n'=0}^{\infty}\Gamma_{nn'}a_n(t) \equiv -\sum_{n'=0}^{\infty}W_{nn'}a_{n'}(t). \quad (17)$$

The Laplace transform (Eq. (9)) of this last equation is

$$(-i\tilde{\omega} + W)a(\tilde{\omega}) = \mathbf{1}_0, \quad (18)$$

where the matrix W is defined through equation (17) and the vector $\mathbf{1}_0$ has the components $\delta_{n,0}$ (notice that, from Eq. (7), $a_n(t=0) = \delta_{n,0}$). If S means the matrix diagonalizing W, the resulting spectral profile is (*cf.* Eq. (10))

$$I(\omega) = \pi^{-1}\mathrm{Re}\{a_0(\tilde{\omega})\} = \pi^{-1}\mathrm{Re}\left\{\sum_k \frac{S_{0k}(S^{-1})_{0k}}{-i\tilde{\omega}+D_k}\right\}, \quad (19)$$

where the diagonal D matrix is given by $D = S^{-1}WS$.

Equation (19) will be used in the following to numerically study the role of the Keilson-Storer speed-memory function (Eq. (3)) on the spectral distribution of a given rovibrational line for gas mixtures. This requires the generalization of the kinetic equation (1), explicitly written for pure gases, to this physical situation. Due to its markovian character, the generalization of equation (1) to a mixture of two species (a) and (b) with respective concentrations c and $(1-c)$ is

$$\dot{d}(v,t) = -\Bigg\{c\left[\gamma^{(a)}_{coll}(v) + i\delta^{(a)}_{coll}(v)\right] + (1-c)\left[\gamma^{(b)}_{coll}(v) + i\delta^{(b)}_{coll}(v)\right]\Bigg\}d(v,t) - c\nu^{(a)}\left[d(v,t) - \int_0^{\infty}dv' f^{(a)}(v',v)d(v',t)\right] - (1-c)\nu^{(b)}\left[d(v,t) - \int_0^{\infty}dv' f^{(b)}(v',v)d(v',t)\right], \quad (20)$$

where the exponent indexes (a) and (b) are relative to collisional pairs $(a)-(a)$ and $(a)-(b)$ respectively. Introducing the usual linear combinations

$$\gamma_{coll}(v) = c\gamma^{(a)}_{coll}(v) + (1-c)\gamma^{(b)}_{coll}(v),$$
$$\delta_{coll}(v) = c\delta^{(a)}_{coll}(v) + (1-c)\delta^{(b)}_{coll}(v),$$
$$\nu = c\nu^{(a)} + (1-c)\nu^{(b)}, \quad (21)$$

equation (20) leads straightforwardly to the same formal kinetic equation as equation (1) with the following definition for the speed-memory function of the gas mixture

$$f(v',v) = \nu^{-1}[c\nu^{(a)}f^{(a)}(v',v) + (1-c)\nu^{(b)}f^{(b)}(v',v)]. \quad (22)$$

By using this new definition (22) for the speed-memory function, all the above mathematical procedures for the calculation of the spectral lineshape, through equation (19), remain unchanged for gas mixtures.

3 Numerical study of speed memory effects on lineshape

The numerical calculation of the Q-line profiles for the H_2-Ar gas mixture from the kinetic equation (20) with the KS kernel (Eq. (3)) depends upon the parameters $\gamma^{(H_2)}$ and $\gamma^{(Ar)}$. These two parameters characterize the speed-memory functions $f^{(H_2)}(v',v)$ and $f^{(Ar)}(v',v)$ respectively (*cf.* Eqs. (3) and (22)). Since no inhomogeneous effect was observed [3,26] in pure H_2, the strong collision model can be used [1–3] for the colliding H_2-H_2 pairs, so that $\gamma^{(H_2)} = 0$ and $f^{(H_2)}(v',v) = W_B(v)$. The calculation of $I(\omega)$ from equation (19) requires the determination of the eigenvalues D_k and of the eigenvector components S_{0k} tied to the W matrix defined through equations (15) and (17). This determination involves calculating the matrices $I^{(p)}_{nn'}(\alpha)$ (Eq. (14)) for the pertinent α values (*i.e.* $\alpha^{(H_2)} = 1$, $\alpha^{(Ar)} = 19.82$) and for $r = 0$ and $s = 1$ (*cf.* Eqs. (11) and (12)) since only the v-dependence of the collisional shift, exhibiting a linear variation with $\sqrt{T}$, has to be considered at room temperature (*cf.* Refs. [3,5,25]). Furthermore, the W matrix has been truncated at $n = 40$ (*cf.* Eq. (17)) in order to ensure convergence up to $\gamma^{(Ar)} = 0.95$. Notice that, for $\gamma = 1$, the analytical asymptotic limit $\delta(v'-v)$ for the KS memory function (Eq. (3)) can be used to easily perform the numerical calculation. All the numerical values for the needed parameters have been taken from reference [3] ($\left(\gamma^{(H_2)}_{coll}\right)_0 = \overline{\gamma}^{(H_2)}_{coll}(295\text{ K}) = 0.87$ mK/amagat, $\left(\gamma^{(Ar)}_{coll}\right)_0 = \overline{\gamma}^{(Ar)}_{coll}(295\text{ K}) = 2.35$ mK/amagat, $\left(\overline{\delta}^{(H_2)}_{coll}\right)_0 = -17.41$ mK/amagat, $\left(\overline{\delta}^{(Ar)}_{coll}\right)_0 = -26.11$ mK/amagat, $\overline{\delta}^{(H_2)}_{coll}(295\text{ K}) = -3.32$ mK/amagat, $\overline{\delta}^{(Ar)}_{coll}(295\text{ K}) = -11.82$ mK/amagat, $\nu^{(H_2)} = 47$ mK/amagat and $\nu^{(Ar)} = 92$ mK/amagat, where 1 mK=10^{-3} cm^{-1} and the amagat is the density unit).

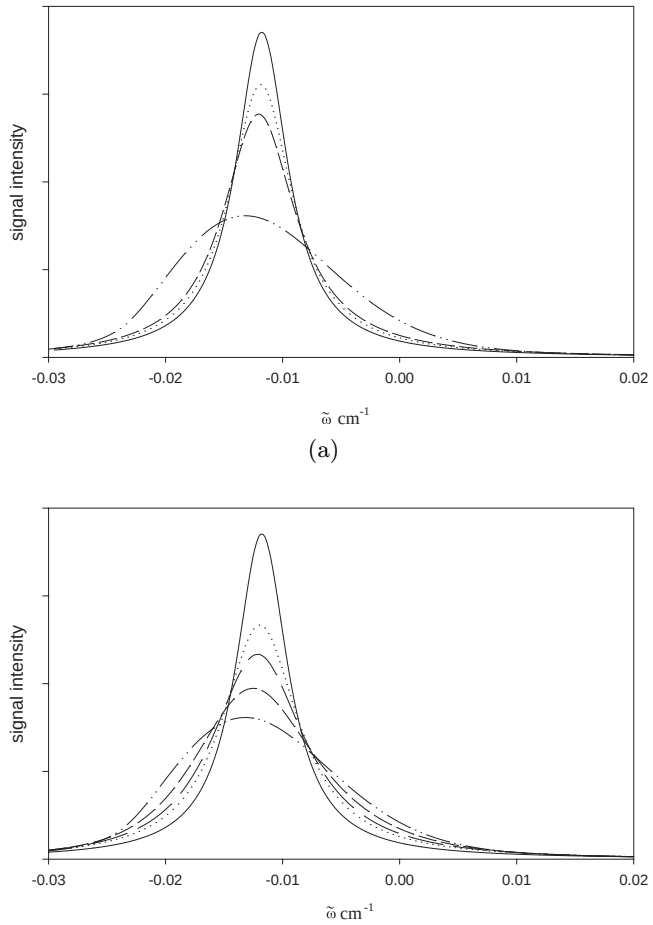

Fig. 1. (a) Isotropic Raman $Q(1)$-line profile $I(\tilde{\omega})$ (in arbitrary units) for H_2 infinitely diluted in argon ($c \to 0$) at $T = 295$ K calculated from the kinetic equation (20) with the KS memory function (Eq. (3)); $\gamma^{(\mathrm{Ar})} = 0$ (———); $\gamma^{(\mathrm{Ar})} = 0.8$ (· · · · · · · · ·); $\gamma^{(\mathrm{Ar})} = 0.95$ (— — —); $\gamma^{(\mathrm{Ar})} = 1$ (— ·· — ·· —). (b) Same as Figure 1a but for the LKS memory function (Eq. (24)). In addition, the case $\tilde{\gamma}^{(\mathrm{Ar})} = 0.88$ (—— —— ——), corresponding to the best fit [3] with experimental data is also given. (Notice that $\tilde{\gamma} = 1-x$ (*cf.* Eq. (28)) where x is the ratio of SC collisions in the SC + D hard collision model; *cf.* Ref. [2]).

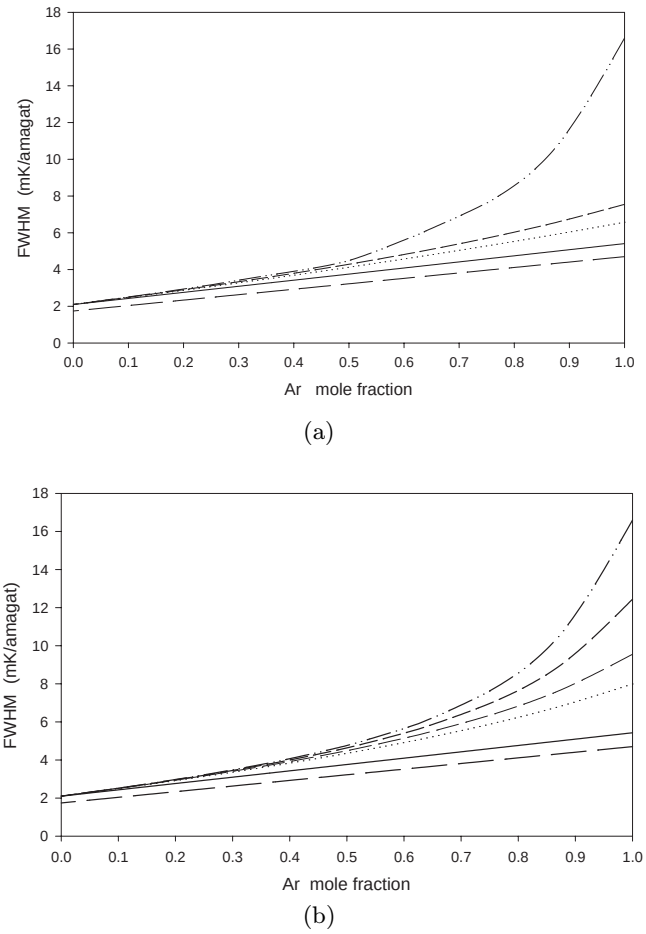

Fig. 2. (a) Isotropic Raman $Q(1)$-line width Γ (FWHM) for H_2-Ar gas mixtures *vs.* argon concentration at $T = 295$ K calculated from the kinetic equation (20) with the KS memory function (Eq. (3)); $\gamma^{(\mathrm{Ar})} = 0$ (———); $\gamma^{(\mathrm{Ar})} = 0.8$ (· · · · · · · · ·); $\gamma^{(\mathrm{Ar})} = 0.95$ (— — —); $\gamma^{(\mathrm{Ar})} = 1$ (— ·· — ·· —). The lowest curve (—— ——) corresponds to the usual linear variation (v-averaged Eq. (21); *cf.* Eq. (13)). (b) Same as Figure 2a but for the LKS memory function (Eq. (24)) including, in addition, the case $\tilde{\gamma}^{(\mathrm{Ar})} = 0.88$ (—— —— ——) (*cf.* Fig. 1b caption).

The resulting effect of the KS speed-memory function on the lineshape is illustrated in Figure 1a for the $Q(1)$-line of H_2 at very high dilution in argon for $T = 295$ K. Following the values of the parameter $\gamma^{(\mathrm{Ar})}$ (*cf.* Eq. (3)), the lineshape varies from a strongly inhomogeneous asymmetric profile (for $\gamma = 1$) to a quasi-homogeneous symmetric one (for $\gamma = 0$). The interpretation of this behavior is made easier by considering the two limits $\gamma = 1$ and $\gamma = 0$. In the soft ($\gamma = 1$) collision limit, the speed-memory is kept after an infinite number of collisions and speed-class exchanges do *not* take place [17]. In the hard collision limit ($\gamma = 0$), the speed-class exchanges have the maximum efficiency since the speed-memory is lost after each collision, resulting in a coalesced spectral lineshape. For intermediate values of γ between 1 and 0, partial correlation of speed leads to increasing speed-class exchanges and, thus, to an increasing coalescence. It is worth noting that these exchanges are efficient for a large range of γ values since the inhomogeneous effects only appear (*cf.* Fig. 1a) for a restricted range of $\gamma (0.8 \lesssim \gamma \leq 1)$.

The variations of the three main characteristics of the spectral profile (*i.e.* the full width Γ, the shift Δ and the asymmetry A) *vs.* the concentration of the mixture for various values of $\gamma^{(\mathrm{Ar})}$ are shown in Figures 2a, 3a and 4a. In Figure 2a, a linear behavior of Γ *vs.* $(1-c)$ Argon mole fraction for $\gamma^{(\mathrm{Ar})} = 0$, is obtained. It slightly differs from the usual linear law ($\gamma_{coll} = c\gamma_{coll}^{(\mathrm{H_2})} + (1-c)\gamma_{coll}^{(\mathrm{Ar})}$). The origin of this difference was explained [2,3] by the fact that in the VC + D hard collision model the collapse of the various speed classes can not be complete, in

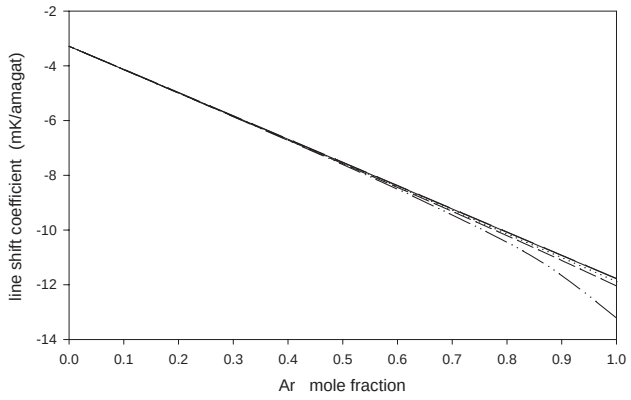

(a)

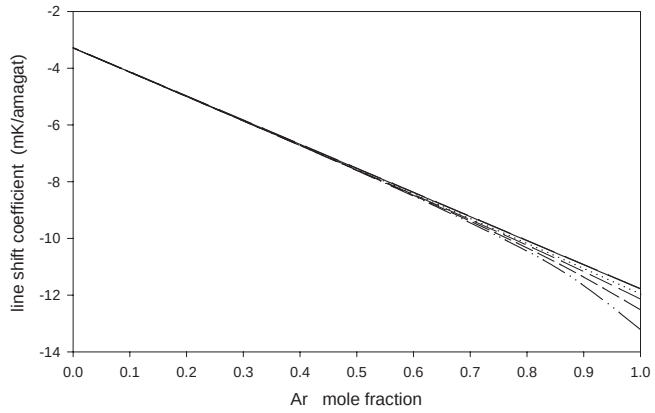

(b)

Fig. 3. (a) Isotropic Raman $Q(1)$-line shift Δ ($\omega = \omega_0 + \Delta$) for H_2−Ar gas mixtures *vs.* argon concentration at $T = 295$ K calculated from the kinetic equation (20) with the KS memory function (Eq. (3)); $\gamma^{(\mathrm{Ar})} = 0$ (———); $\gamma^{(\mathrm{Ar})} = 0.8$ (· · · · · · · · ·); $\gamma^{(\mathrm{Ar})} = 0.95$ (— — —); $\gamma^{(\mathrm{Ar})} = 1$ (— ·· — ·· —). Notice that the $\gamma = 0$ curve coincides with the usual linear variation (v-averaged Eq. (21)). (b) Same as Figure 3a but for the LKS memory function (Eq. (24)) including, in addition, the case $\tilde{\gamma}^{(\mathrm{Ar})} = 0.88$ (—— —— ——) (*cf.* Fig. 1b).

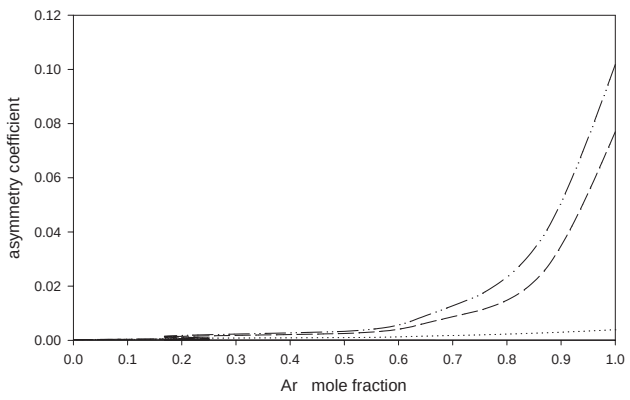

(a)

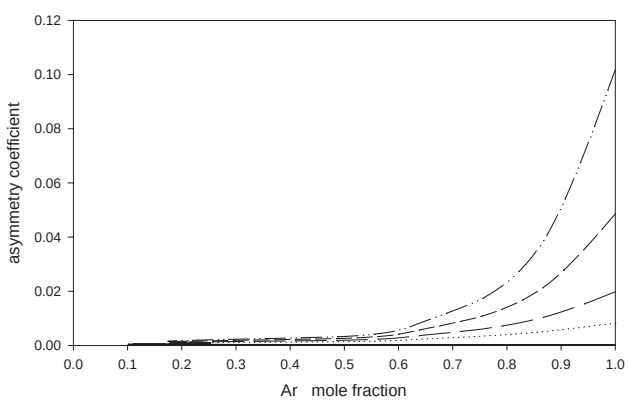

(b)

Fig. 4. (a) Isotropic Raman $Q(1)$-line asymmetry $A = [\nu_{HF} + \nu_{LF} - 2\nu_{Max}]/\Gamma$ (where ν_{HF} and ν_{LF} means the high and low frequencies at half maximum respectively, ν_{Max} is the maximum frequency and Γ the FWHM) for H_2 infinitely diluted in argon ($c \to 0$) at $T = 295$ K calculated from the kinetic equation (20) with the KS memory function (Eq. (3)); $\gamma^{(\mathrm{Ar})} = 0$ (———); $\gamma^{(\mathrm{Ar})} = 0.8$ (· · · · · · · · ·); $\gamma^{(\mathrm{Ar})} = 0.95$ (— — —); $\gamma^{(\mathrm{Ar})} = 1$ (— ·· — ·· —) (the $\gamma^{(\mathrm{Ar})} = 0$ curve is very close to zero and almost superposed to the argon-concentration axis). (b) Same as Figure 4a but for the KS memory function (Eq. (24)) including, in addition, the case $\gamma^{(\mathrm{Ar})} = 0.88$ (—— —— ——) (*cf.* Fig. 1b).

contrast with the partially correlated VCD +D hard collision model. This results in a weak residual inhomogeneous contribution, less than one mK/amagat. The second important feature in Figure 2a, is the weak inhomogeneous broadening for $c > 0.5$, whatever the KS memory parameter $\gamma^{(\mathrm{Ar})}$. This inhomogeneous broadening is only efficient for weak H_2-concentration and for a $\gamma^{(\mathrm{Ar})}$ parameter close to one (typically between 0.8 and 1) where a drastic non-linear increase of Γ is observed. For the shift Δ (Fig. 3a), the role of the concentration is also important and the inhomogeneous shifting effect is less important than for the broadening. The residual inhomogeneity between the linear variation for $\gamma^{(\mathrm{Ar})} = 0$ and the usual linear law ($\delta_{coll} = c\delta_{coll}^{(\mathrm{H_2})} + (1-c)\delta_{coll}^{(\mathrm{Ar})}$) is negligible.

For the asymmetry A of the line, which is the third signature of the speed-changing collision effect, the remarks concerning the role of the concentration and $\gamma^{(\mathrm{Ar})}$ are also relevant. The non-linear behavior of A *vs.* $\gamma^{(\mathrm{Ar})}$ is even more pronounced than for Γ.

As a whole, these three Figures 2a, 3a and 4a show the crucial role played by the weak collisions in the resulting inhomogeneous features of the line profile. This point will be used in the following section (Sect. 4) through an alternative analytical model based on a linearized Keilson-Storer memory function.

4 An analytical expression for the lineshape from a simplified model for the speed-memory function

The numerical solution of the impact kinetic equation (1) using the speed-memory Keilson-Storer model [18] has allowed us to get a clear understanding of the basic mechanism underlying the speed-changing collisional effects on the spectral lineshape. Particular interest lies in an analytical expression for the spectral lineshape for practical applications in atmospheric sciences or in diagnostics of combustion media. Furthermore such an analytical expression should permit the establishment of a connection between the present approach using the KS memory function and the useful and efficient hard collision model [1,2]. For this reason, we introduce now an alternative realistic speed-memory function.

The KS function (Eq. (2)) gives the simple analytical limits for $\gamma = 0$ and $\gamma = 1$,

$$f_0^{KS}(\mathbf{v}', \mathbf{v}) = W_B(\mathbf{v}),\ f_1^{KS}(\mathbf{v}', \mathbf{v}) = \delta(\mathbf{v}' - \mathbf{v}). \quad (23)$$

Therefore, after averaging over the $\mathbf{v}$-orientation, a model for $f(v', v)$, still satisfying detailed balance, may be obtained by using a linearized KS (LKS) model

$$f(v', v) = (1 - \tilde{\gamma})W_B(v) + \tilde{\gamma}\delta(v' - v), \quad (24)$$

where $\tilde{\gamma}$ is the *fraction of soft collisions* in an ensemble of collisions including *only* hard ($\gamma = 0$) and soft ($\gamma = 1$) collisions. In such an LKS model, the $\tilde{\gamma}$-weighted statistical mixing of the two types of collisions (24) is substituted for the KS memory function (3). Let us recall that this last function is tied to a *given* colliding pair accounting for all possible statistical behaviors through the KS parameter γ. Substituting equation (24) in equation (1) gives the kinetic equation

$$\dot{d}(v,t) = -[\gamma_{coll}(v) + i\delta_{coll}(v)]d(v,t) - (1 - \tilde{\gamma})\nu^{VC}\left[d(v,t) - W_B(v)\int_0^\infty dv' d(v',t)\right]. \quad (25)$$

The Laplace transform of this equation leads straightforwardly from equation (10) to the following expression for the spectral lineshape for the case of *statistical independent* VC and D collisions (VC+D)

$$I(\tilde{\omega}) = \frac{\varphi^{WSL}_{(1-\tilde{\gamma})\nu^{VC}}(\tilde{\omega})}{1 - (1 - \tilde{\gamma})\nu^{VC}\varphi^{WSL}_{(1-\tilde{\gamma})\nu^{VC}}(\tilde{\omega})}, \quad (26)$$

where the Weighted Sum of Lorentzian (WSL) function is defined by

$$\varphi^{WSL}_{\nu}(\tilde{\omega}) = \int_0^\infty dv \frac{W_B(v)}{\nu + \gamma(v) - i[\tilde{\omega} - \delta(v)]}. \quad (27)$$

Equation (26) is *formally identical* to the SC+D hard collision model [1,2] through the following correspondence between ν^{SC} and ν^{VC},

$$\nu^{SC} = (1 - \tilde{\gamma})\nu^{VC}. \quad (28)$$

This relation shows that the connection between the velocity-changing frequency ν^{VC} used to treat the collisional (HC) effects in the Doppler regime [12] and the speed-changing frequency ν^{SC} introduced in the collisional one [1,2], is the direct consequence of the speed-memory effect. Within the frame of the present LKS model (Eq. (24)), this last effect results in the phenomenological $(1 - \tilde{\gamma})$ factor in equation (28).

It is interesting to analyze the lineshape behavior within the LKS frame (or equivalently for the SC+D (HC) model of Ref. [1] through Eq. (28)). Figures 1b to 4b display the resulting lineshape features for the same example used in the above analysis of the KS memory effects. This permits a direct comparison between the two types of memory functions (KS and LKS). Figure 1b shows that the behavior of the $Q(1)$-line profile for H_2 at very low dilution in Argon for $T = 295$ K is close to that obtained with the KS model (*cf.* Fig. 1a). A more detailed analysis, through the three characteristic parameters Γ, Δ and A (Figs. 2b to 4b) confirms this statement. Of course, the resulting profiles for the two different memory functions (KS and LKS) present significant numerical discrepancies but all the above general comments concerning Figures 2a to 4a remain relevant.

Let us recall that the profiles obtained from the solution (26) of the kinetic equation (25) with the LKS memory function (24) are identical to that obtained from the SC + D model [1] based on the hard collision approximation (*i.e. without* memory process). In this last model, the memory effect is in fact accounted for through the phenomenological ν^{SC} parameter (*cf.* Eq. (28)).

5 Conclusion

A kinetic model based on the Keilson-Storer memory function [18] has been used to analyze the influence of the speed-changing collisions on spectral lineshapes. The parameter γ characterizing the KS memory function has been shown to play a crucial role through the speed-class exchanges. These exchanges strongly modify the inhomogeneous distribution resulting from the speed-dependence of the broadening and shifting parameters.

The numerical solution of the kinetic equation for VC + D collisions with the KS kernel leads to line profiles lying between a weighted sum of Lorentzian inhomogeneous asymmetric profiles (for soft collisions ($\gamma = 1$)) and a quasi-homogeneous symmetric profile (for hard collisions ($\gamma = 0$)). The collisionally induced speed-class exchanges partially cancel this inhomogeneous distribution. The calculated profiles present the expected experimental features, *i.e.* a non-linear dependence of the line broadening and of the line shifting parameters on perturber concentration, as well as an asymmetry depending on this concentration.

An alternative linearized Keilson-Storer (LKS) model for the memory function has allowed us to deduce an analytical expression for the lineshape accounting for the speed- memory effects. This expression is formally identical to that previously obtained [1] in the hard collision

approximation and successfully used to quantitatively analyze the observed spectral features in H_2-Ar mixtures in a wide temperature range. Their identification leads to a relation between the velocity-changing collision frequency ν^{VC} and the speed-changing one ν^{SC} through a parameter. This parameter is the fraction of soft ($\gamma = 1$) collisions in the simplified LKS memory function model, which only accounts for two types (hard and soft) of collisions. This fully clarifies the meaning of ν^{SC} in the VC + D (HC) model. This collision speed-changing rate ν^{SC} phenomenologically accounts for the speed-memory effect.

Furthermore, this relation between ν^{VC} and ν^{SC} establishes a bridge between two distinct approaches, that of the Dicke narrowing , through the velocity-changing collisions, in the Doppler regime (low density), and that of inhomogeneous effects though the speed- dependence of the broadening and shifting parameters in the collision regime (high density). In the present paper (I), only this last regime has been considered for the sake of clarity. The introduction of the Doppler contribution in the kinetic model used here and its exact numerical resolution with the 3D Keilson-Storer (instead of 1D as used here) memory function [18] will be considered in the next paper (II).

References

1. R.L. Farrow, L.A. Rahn, G.O. Sitz, G.J. Rosasco, Phys. Rev. Lett. **63**, 746 (1989).
2. D. Robert, J.M. Thuet, J. Bonamy, S. Temkin, Phys. Rev. A **47**, R771 (1993).
3. J. Ph. Berger, R. Saint-Loup, H. Berger, J. Bonamy, D. Robert, Phys. Rev. A **49**, 3396 (1994).
4. J.W. Forsman, J. Bonamy, D. Robert, J.Ph. Berger, R. Saint-Loup, H. Berger, Phys. Rev. A **52**, 2652 (1995).
5. P.M. Sinclair, J.Ph. Berger, X. Michaut, R. Saint-Loup, R. Chaux, H. Berger, J. Bonamy, D. Robert, Phys. Rev. A **54**, 402 (1996).
6. E.P. Gross, Phys. Rev. **97**, 395 (1955).
7. M. Nelkin, A. Ghatak, Phys. Rev. **135**, A4 (1964).
8. P.L. Varghese, R.K. Hanson, Appl. Optics **23**, 2376 (1984).
9. M. Henry, D. Hurtmans, M. Margottin-Maclou, A. Valentin, J. Quant. Spectrosc. Radiat. Trans. **56**, 647 (1996) and references cited therein.
10. A.S. Pine, J. Chem. Phys. **101**, 3444 (1994) and references cited therein.
11. B. Lance, G. Blanquet, J. Walrand, J.P. Bouanich, J. Mol. Spectrosc. **185**, 262 (1997).
12. S.G. Rautian, I.I. Sobel'man, Soviet. Phys. Uspekhi **9**, 701 (1967).
13. P. Duggan, P.P. Sinclair, A.D. May, J.R. Drummond, Phys. Rev. A **51**, 218 (1995).
14. P.M. Berman, J. Quant. Spectrosc. Radiat. Trans. **12**, 1331 (1972).
15. G. Nienhuis, J. Quant. Spectrosc. Radiat. Trans. **20**, 275 (1978).
16. L. Galatry, Phys. Rev. **122**, 1218 (1961).
17. R. Ciurylo, J. Szudy, J. Quant. Spectrosc. Radiat. Trans. **57**, 411 (1997).
18. J. Keilson, J.E. Storer, Quarterly Appl. Math. **10**, 243 (1952).
19. A.B. Doktorov, A.I. Burshtein, Sov. Phys. JETP **36**, 411 (1973).
20. A.J. Burshtein, A.G. Kofman, Sov. Phys. JETP **43**, 436 (1976).
21. A.I. Burshtein, S.I. Temkin, Sov. Phys. JETP **44**, 492 (1976).
22. A.I. Burshtein, S.I. Temkin, *Spectroscopy of Molecular rotation in gases and liquids* (Cambridge University Press, 1994).
23. M. Abramowitz, I.A. Stegun, *Handbook of Mathematical functions* (Dover Publications Inc., New York, 1970).
24. H.M. Pickett, J. Chem. Phys. **73**, 6090 (1980).
25. J.Ph. Berger, Ph.D. Thesis, Dijon (1994).
26. L.A. Rahn, G.J. Rosasco, Phys. Rev. A **41**, 3698 (1990).